JCB Article

Focal loss of actin bundles causes microtubule redistribution and growth cone turning

Feng-Quan Zhou,[1] Clare M. Waterman-Storer,[2] and Christopher S. Cohan[1]

[1]Department of Anatomy and Cell Biology, University at Buffalo, SUNY, Buffalo, NY 14214
[2]Department of Cell Biology, The Scripps Research Institute, La Jolla, CA 92037

It is commonly believed that growth cone turning during pathfinding is initiated by reorganization of actin filaments in response to guidance cues, which then affects microtubule structure to complete the turning process. However, a major unanswered question is how changes in actin cytoskeleton are induced by guidance cues and how these changes are then translated into microtubule rearrangement. Here, we report that local and specific disruption of actin bundles from the growth cone peripheral domain induced repulsive growth cone turning. Meanwhile, dynamic microtubules within the peripheral domain were oriented into areas where actin bundles remained and were lost from areas where actin bundles disappeared. This resulted in directional microtubule extension leading to axon bending and growth cone turning. In addition, this local actin bundle loss coincided with localized growth cone collapse, as well as asymmetrical lamellipodial protrusion. Our results provide direct evidence, for the first time, that regional actin bundle reorganization can steer the growth cone by coordinating actin reorganization with microtubule dynamics. This suggests that actin bundles can be potential targets of signaling pathways downstream of guidance cues, providing a mechanism for coupling changes in leading edge actin with microtubules at the central domain during turning.

Introduction

Growth cones at the growing tips of the axon play a critical role in controlling axon pathfinding by responding to extracellular guidance cues (Tessier-Lavigne and Goodman, 1996). Actin filaments are major cytoskeletal elements that determine the structure of growth cones (Letourneau, 1983; Gordon-Weeks, 1987). An actin meshwork is concentrated at the leading edge of the growth cone and actin bundles project radially through the growth cone into the filopodia (Bentley and O'Connor, 1994). Microtubules are the other major structural elements of growth cones. They project from the axon shaft to the central area (C-domain)* of the growth cone with their dynamic ends splaying apart and invading into the actin-rich peripheral area (P-domain). Precise pathfinding by axonal growth cones depends on continuous reorganization of their cytoskeletal structures, including both actin filaments and microtubules (Tanaka and Sabry, 1995), in response to guidance cues. However, how growth cones translate guidance signals into directed axonal growth is mostly unknown (Song and Poo, 1999; Suter and Forscher, 2000). A key to understanding this is to define how changes in F-actin in growth cones are coordinated with changes in microtubules in response to guidance cues.

Studies have indicated that when growth cones turn toward attractive cues, either a target cell or nerve growth factor beads, F-actin rapidly becomes concentrated at the site where the growth cone will turn, followed by lamellipodial protrusion in that direction, as well as asymmetrical microtubule advancement into the peripheral area of the growth cone where actin accumulation occurs (Lin and Forscher, 1993; Gallo and Letourneau, 2000). On contact with repulsive cues, it is believed that asymmetric growth cone collapse leads to repulsive growth cone turning (Fan and Raper, 1995). For instance, a brain-derived repulsive factor (collapsin) has been shown to cause loss of F-actin from the growth cone leading edge (Fan et al., 1993). In addition, Challacombe et al. (1996) have shown that dynamic microtubule ends are rearranged within growth cones to avoid an inhibitory guidance cue. Although these studies suggest the involvement of actin and microtubule reorganization during growth cone

The online version of this manuscript contains supplemental material.

Address correspondence to Dr. Christopher S. Cohan, Department of Anatomy and Cell Biology, University at Buffalo, Buffalo, NY 14214. Tel.: (716) 829-3081. Fax: (716) 829-2911. E-mail: ccohan@buffalo.edu

F.-Q. Zhou's present address is Neuroscience Center, University of North Carolina at Chapel Hill, Chapel Hill, NC 27599.

*Abbreviations used in this paper: AFI, average fluorescent intensity; BDM, 2,3-butanedione monoxime; C-domain, central domain; FSM, fluorescent speckle microscopy; LPA, lysophosphatidic acid; MLCK, myosin light chain kinase; ML-7, 1-(5-iodonaphthalene-1-sulfonyl)-1H-hexahydro-1,4-diazepine-HCl; P-domain, peripheral domain.

Key words: axon guidance; pathfinding; actin bundles; cytoskeleton; microtubules

turning, no direct evidence exists to explain how F-actin is regulated during turning and how F-actin and microtubule reorganization is coordinated. Thus, identifying potential cytoskeletal events during turning will be crucial to unravel this question.

We have developed a model system using two different preparations of *Helisoma* neurons to study cytoskeletal mechanisms of growth cones in response to repulsive guidance cues. In brief, when *Helisoma* neurons are cultured in conditioned medium, they form typical, motile growth cones that grow, collapse, and turn (Cohan et al., 1987). In contrast, neurons cultured on polylysine-coated coverslips in the absence of conditioned medium form larger, nonmotile growth cones (Welnhofer et al., 1997) that do not collapse due to increased membrane adhesion (Zhou and Cohan, 2001). These polylysine-attached growth cones allow observation of cytoskeletal changes that are difficult in extending growth cones. By using this model, we previously showed that actin bundle loss is a common cytoskeletal event mediating growth cone collapse (Zhou and Cohan, 2001) through regulating leading edge actin organization. In this study, we tested whether regional loss of actin bundles affected microtubule organization and growth cone steering. We found that local application of a collapsing factor induced actin bundle loss on one side of growth cones, which resulted in selective exclusion of microtubules from that side and repulsive turning away from the stimulus. We provide direct evidence that most microtubule free ends are restricted from the peripheral domain by the influence of retrograde flow of actin meshwork, but not by actin meshwork alone. Furthermore, actin bundles provide the means by which a small subset of microtubules overcome retrograde flow and extend toward the leading edge. We also show that local actin bundle loss and asymmetric protrusion precede microtubule changes and growth cone turning. Together, our results suggest that actin bundles may be key cytoskeletal targets of physiological guidance cues, which could mediate growth cone turning by coordinating actin dynamics at the leading edge with microtubule dynamics near the central domain.

Results

Local actin bundle loss causes repulsive growth cone turning

Repulsive factors cause collapse of growth cones when they are bath applied to neuronal cultures or they can cause turning of growth cones when they are applied more focally by pipettes positioned near growth cones. Because collapsing factors have been shown to act by eliminating actin bundles (Zhou and Cohan, 2001), we tested whether a local loss of actin bundles in growth cones induced turning. We used 1-(5-iodonaphthalene-1-sulfonyl)-1H-hexahydro-1,4-diazepine-HCl (ML-7), a specific myosin light chain kinase (MLCK) inhibitor, which acts only on actin bundles without disrupting actin meshwork through inactivation of myosin II (Bridgman et al., 2001; Zhou and Cohan, 2001). We first tested whether factors that caused actin bundle loss could induce repulsive turning of extending conditioned medium growth cones when locally applied. To produce a local effect, a microscopic gradient of solution near growth cones was created by repetitively releasing ML-7 (100 μM) or control solution (2% DMSO in medium) from a micropipette (Song et al., 1997). After a 1-h application of gradient, we observed a marked and consistent repulsive turning response of growth cones in response to ML-7 (Fig. 1, a and d; turning angle = −23.29 ± 5.21; $P < 0.01$). Control growth cones showed no apparent bias in turning (Fig. 1, b and d; turning angle = −1.52 ± 5.23). To further confirm the repulsive effect of ML-7, some double turning experiments were done, in which growth cone turning in one direction was reversed by repositioning the pipette after the first turn (Fig. 1 c). Previously, we showed that lysophosphatidic acid (LPA) was able

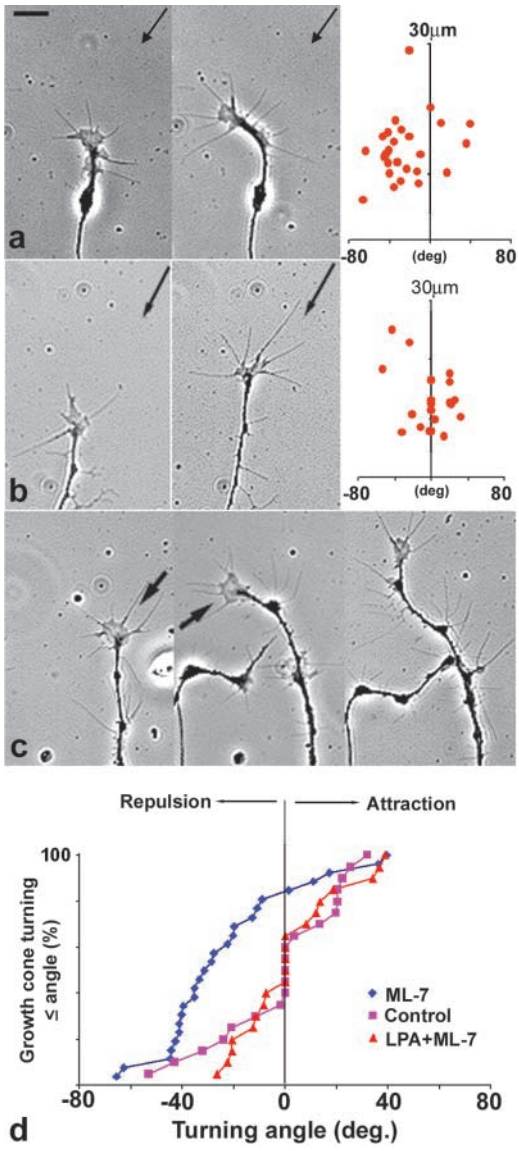

Figure 1. **Local application of collapsing factor (ML-7) causes repulsive growth cone turning.** (a) A growth cone turned away from ML-7 gradient after 1 h (arrow indicates the direction of pipette). Scatter plots of turning angle and neurite extension indicate preference of repulsive turning ($n = 26$). (b) A control growth cone at the beginning and end of 60 min of DMSO gradient. Scatter plots indicate no bias in growth cone turning ($n = 20$). (c) A growth cone turned away from ML-7 twice after the pipette was repositioned (arrows). (d) Cumulative distribution of turning angles. Note that LPA pretreatment abolished repulsive turning induced by ML-7 ($n = 20$). Bar, 10 μm.

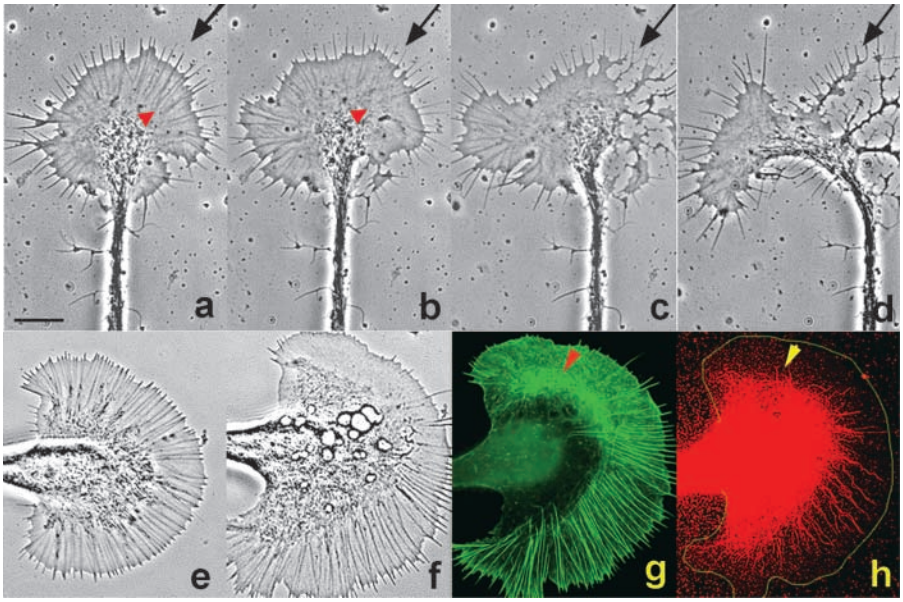

Figure 2. **Local actin bundle loss induces growth cone turning.** Larger extending conditioned medium growth cones (a–d) have more prominent actin bundles (a) similar to that of polylysine-attached growth cones (e). Local application of ML-7 (arrows indicate the position of pipette) induced local actin bundle loss (a and b, red arrowheads), followed by local lamellipodia collapse (c). Meanwhile, asymmetrical lamellipodial protrusion occurred in the area where actin bundles remained (c). Finally, microtubules extended in the direction of lamellipodial protrusion and consolidated to complete the turning process (d). To show cytoskeletal reorganization after local actin bundle loss in the absence of collapse, polylysine-attached growth cones were used (e–h). Local actin bundle loss induced asymmetrical lamellipodial protrusion similar to that shown in Fig. 2 (c). Phalloidin staining showed local translocation of F-actin from the leading edge to the center in the area where actin bundle loss occurred (g, arrowhead). In the meantime, microtubule staining showed that free microtubule ends were also abolished from the corresponding area where actin bundles were absent (h, arrowhead). Bar, 10 μm.

to antagonize actin bundle loss and growth collapse caused by ML-7 (Zhou and Cohan, 2001). Similarly, pretreatment with LPA significantly abolished the repulsive turning response by ML-7 (Fig. 1 d; turning angle = 1.59 ± 4.35). All three treatments had no significant effect on the neurite extension rate (13.36 ± 1.12 μm/h in control; 13.88 ± 0.92 in ML-7; 10.44 ± 1.06 in LPA + ML-7). Our results indicate that ML-7, which specifically induces actin bundle loss and whole growth cone collapse when bath applied (Zhou and Cohan, 2001), is able to induce repulsive turning when applied locally, presumably mediated by local actin bundle loss and subsequent partial growth cone collapse.

Fortunately, larger conditioned medium growth cones allowed us to directly test whether local actin bundle loss is responsible for the turning shown above. As shown in Fig. 2 a, these conditioned medium growth cones have prominent actin bundles similar to that of polylysine-attached growth cones. However, they are motile and collapse when contacting collapsing factors (Zhou and Cohan, 2001). Local application of ML-7 on these growth cones induced local actin bundle loss (Fig. 2 b), followed by partial growth cone collapse and asymmetrical lamellipodial protrusion (Fig. 2 c). Finally, it led to directional microtubule extension and the whole growth cone turning away from the ML-7 source (Fig. 2 d). This directly showed that actin bundle loss preceded repulsive growth cone turning, indicating its underlying role for the turning. This is also the first explicit demonstration that turning results from partial collapse of the growth cone.

Microtubule reorganization in response to actin bundle loss

To show how growth cone cytoskeletal structures reorganized after local application of ML-7, we examined polylysine-attached growth cones in the absence of partial collapse. Release of ML-7 from the pipette caused a local loss of actin bundles on the same side of the growth cone, but no loss of actin meshwork (Fig. 2, e–g), confirming the local effect. This also was accompanied by local decrease of actin accumulation at the leading edge, which may underlie subsequent localized collapse (Fig. 2 g), consistent with our previous finding (Zhou and Cohan, 2001). Meanwhile, when microtubules in the P-domain were examined, we found that they were absent in areas where actin bundles were lost, but they were present in areas where actin bundles still remained (Fig. 2 h), suggesting a role of actin bundles in initiating directional microtubule extension by orienting microtubule ends in the P-domain. Together, this provides direct evidence that actin bundles can coordinate actin reorganization at the leading edge with microtubule organization near the central domain, both of which are required for growth cone turning (Challacombe et al., 1996, 1997; Williamson et al., 1996).

To further study how actin bundle loss regulates microtubule organization, control polylysine-attached growth cones and polylysine-attached growth cones that had lost all their actin bundles after treatment with ML-7 were examined because they retain spread lamellipodia even in the absence of the cytoskeleton. In control growth cones, free dynamic microtubule ends that stained with tyrosinated tubulin antibody protruded into the P-domain and overlapped with actin bundles (Fig. 3, a and b; Gordon-Weeks, 1991). More stable microtubules that stained with an acetylated tubulin antibody were present in the axon and C-domain but not in the P-domain. However, growth cones without actin bundles after ML-7 treatment, but which retained the actin meshwork, were devoid of dynamic microtubule ends inside their F-actin–rich domain (Fig. 3, e and f), suggesting a role for actin bundles in regulating spatial distribution of dynamic microtubules in the P-domain. The result that a different stimulus, serotonin, which also causes actin bundle loss (Zhou and Cohan, 2001), induced the same microtubule exclusion (Fig. 3, i and j) further confirmed this role and suggested the physiological importance of these changes.

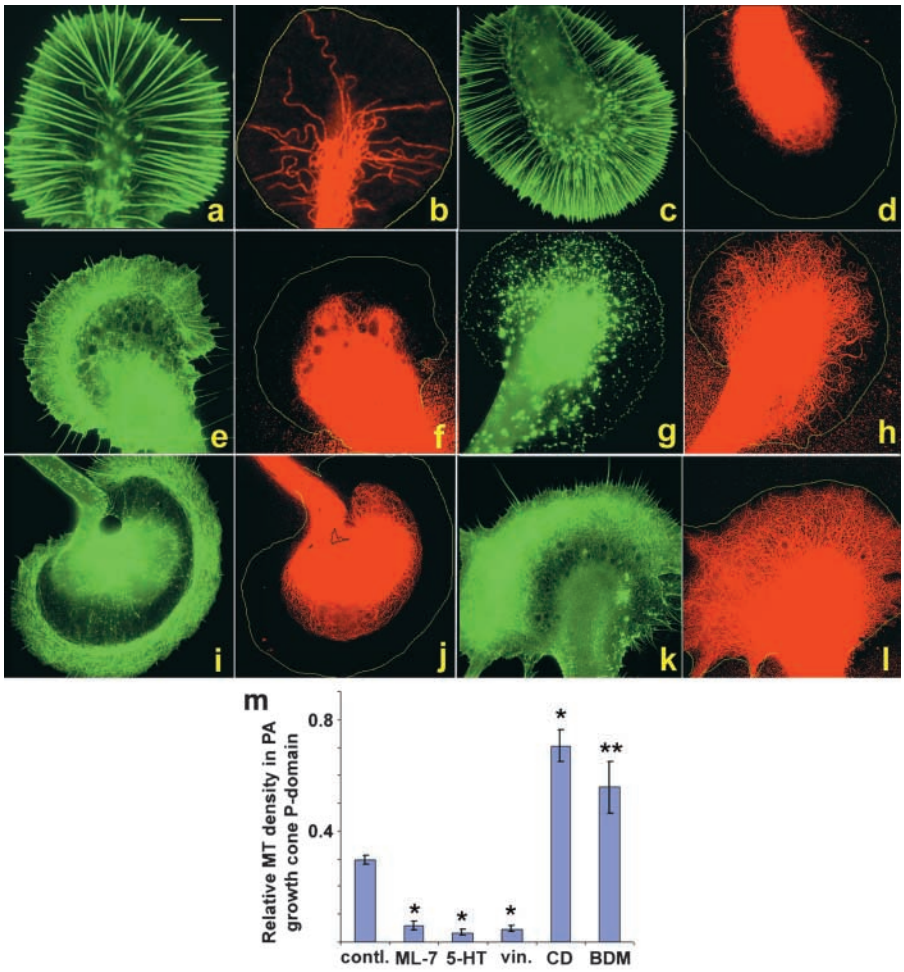

Figure 3. **Effects of actin bundle loss on microtubule organization in polylysine-attached growth cones.** In control polylysine-attached growth cones that have prominent actin bundles (a), many single dynamic microtubule free ends can be seen to extend into the actin-rich P-domain (b), some of which overlap with actin bundles. Growth cones treated with ML-7 lost all their actin bundles, but actin meshwork still remained (e). Microtubule staining showed that free microtubule ends were totally abolished from the P-domain (f) compared with the control. Serotonin (5-HT) that also causes actin bundle loss induced similar microtubule reorganization (i and j). Note that microtubules formed random loops. Vinblastin treatment that abolished free microtubule ends from the P-domain had no effect on actin bundle structures (c and d). Cytochalasin (CD) treatment disorganized F-actin (g) and induced protrusion of microtubules into the growth cone P-domain (h). BDM, similar to ML-7, also induced actin bundle loss without loss of actin meshwork (k), but it also induced protusion into the P-domain (l). Relative microtubule (MT) densities in the polylysine-attached (PA) growth cone actin-rich P-domain were calculated (m). One asterisk indicates a significant difference from control ($P < 0.0001$). Two asterisks indicate $P < 0.05$. Bar, 5 μm.

To show that changes in microtubules themselves cannot cause actin bundle loss, we treated polylysine-attached growth cones with a low concentration of vinblastin (10 nM), which has been shown to delete microtubules from the growth cone P-domain (Challacombe et al., 1997). This had little effect on actin organization even though it depleted all dynamic microtubules from the P-domain (Fig. 3, c and d), further confirming the role of F-actin reorganization in causing microtubule redistribution.

The above findings raised an important question about why microtubules were lost from the P-domain when actin bundles were removed. Under those conditions, the remaining actin meshwork may have had an inhibitory influence on microtubules. Therefore, we tested whether the actin meshwork inhibited microtubule expansion by treatment with cytochalasin D. Cytochalasin D (1 μM) induced a complete loss of actin filaments (Fig. 3 g). When microtubule structure was examined, loss of all actin filaments permitted microtubule free ends to invade the P-domain (Fig. 3 h), which is consistent with a previous study (Forscher and Smith, 1988). However, microtubule invasion might have resulted from either the loss of the actin meshwork itself or, alternatively, the lack of retrograde flow of the actin meshwork, which also is known to influence microtubules (Waterman-Storer and Salmon, 1997). To test whether retrograde flow in the P-domain affected microtubule distribution, we treated growth cones with 2,3-butanedione monoxime (BDM), a myosin ATPase inhibitor that is widely used to inhibit retrograde actin flow (Lin et al., 1996). Unlike ML-7, which inhibits myosin II selectively, BDM inhibits all myosin isoforms. BDM (10 mM) reduced retrograde flow by 49% ($n = 5$ growth cones), but actin meshwork was retained (Fig. 3 k) although actin bundles were lost, as with ML-7. Under these conditions, microtubules expanded into the P-domain, disregarding the presence of the actin meshwork (Fig. 3 l). This demonstrates a role for retrograde flow in regulating microtubule distribution (Waterman-Storer and Salmon, 1997). Quantitative analysis of microtubule ends in the P-domain under each condition is shown in Fig. 3 m. Together, our results indicate that microtubule spatial distribution in the growth cone P-domain is regulated by both F-actin organization and dynamics.

To further confirm the role of F-actin in regulating microtubule distribution, we also examined motile growth cones in conditioned medium. Similar to polylysine-attached growth cones, most control growth cones had dynamic microtubule ends in the P-domain, many of which overlapped with actin bundles (Fig. 4, a and d). However, collapsed growth cones after ML-7 treatment showed few dynamic microtubule ends. Instead, most microtubules in these growth cones formed random loops (Fig. 4, b and e). B19 growth cones that collapsed after serotonin treatment and growth cones that collapsed naturally after long-term culture showed the same result (unpublished data). Growth cones

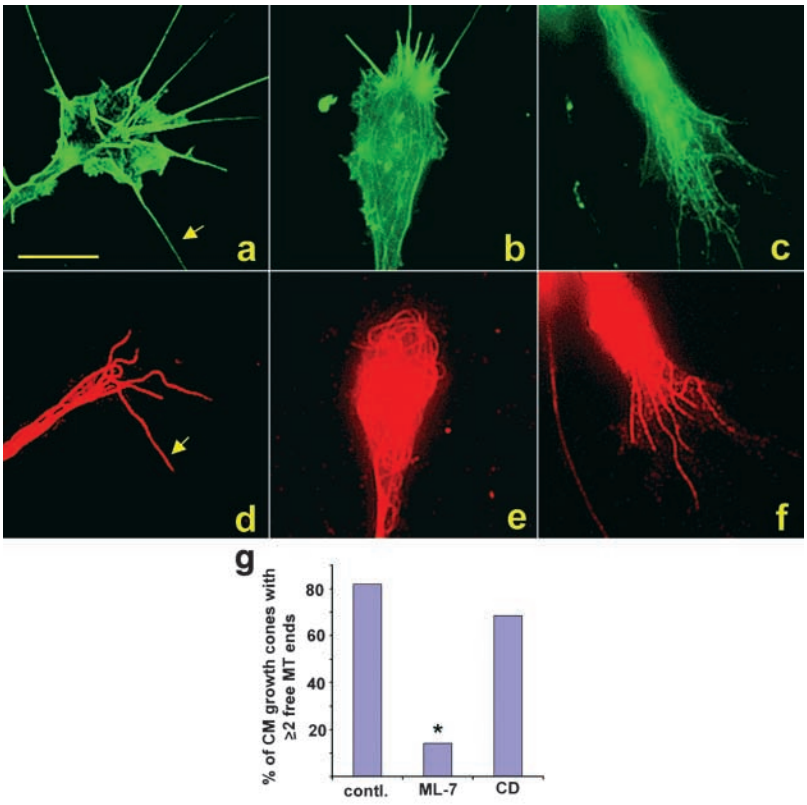

Figure 4. **Microtubule reorganization in conditioned medium growth cones.** A control conditioned medium growth cone showed similar F-actin (a) and microtubule (d) organization to that of polylysine-attached growth cones with microtubule ends extending into the actin-rich P-domain, overlapping and even entering filopodia (a and d, arrows). Growth cone treated with ML-7 retracted its lamellipodia (b). Free microtubule ends were also depleted from the P-domain (e). Instead, microtubules formed random loops that were similar to that of polylysine-attached growth cones. Cytochalasin treatment disorganized F-actin structure (c), but microtubule structure was little changed (f). Percentage of conditioned medium (CM) growth cones with two or more microtubule ends was calculated in each condition (g). Asterisk indicates a significant difference from control ($P < 0.0001$). Bar, 5 μm.

collapsed by cytochalasin showed free microtubule ends similar to those of controls (Fig. 4, c and f). These findings from conditioned medium growth cones (Fig. 4 g) paralleled those from the polylysine-attached growth cones, and show specifically that loss of actin bundles, but not F-actin in general, causes loss of dynamic microtubule free ends in the P-domain.

Measurement of microtubule dynamics in growth cones

We used time-lapse spinning disk confocal fluorescent speckle microscopy (FSM) to characterize the dynamics of microtubules in the growth cone. In FSM imaging, random coincorporation of a few labeled and many endogenous unlabeled tubulin dimers during microtubule assembly gives microtubules a fluorescent speckled appearance in high magnification, diffraction-limited fluorescence images (Waterman-Storer et al., 1998). The fluorescent speckles act as fiduciary marks on microtubules, much like those produced by local photobleaching or fluorescence photoactivation, except with much higher spatial resolution than either of those techniques. In time-lapse FSM, speckle movement reports microtubule movement, whereas appearance or disappearance of linear speckle arrays report microtubule assembly and disassembly.

Using FSM, we found that speckle marks on the lattice of microtubules in the P-domain were continuously transported rearward at 4.13 ± 0.12 μm/min ($n = 139$), similar to the rate of surface-coupled beads (Welnhofer et al., 1997). In addition to this retrograde transport, microtubule plus ends underwent growth and shortening excursions (see supplemental Video 1 available at http://www.jcb.org/cgi/content/full/jcb.200112014/DC1) qualitatively similar to dynamic instability seen in nonneuronal cells (Waterman-Storer and Salmon, 1997). FSM allowed us to monitor the growth of microtubules relative to retrograde flow rates. This revealed that microtubule plus ends grew at a rate of 6.94 ± 0.43 μm/min ($n = 69$ growth rate events). Because the microtubule growth rate was significantly faster than the retrograde flow rate, this allowed growing microtubules to extend toward the leading edge. However, most microtubules were removed from the P-domain due to the small percentage of time that they grew.

Local actin bundle loss induced asymmetrical lamellipodial and central domain protrusion

Growth cone turning has been suggested to involve asymmetrical lamellipodial protrusion (Fan and Raper, 1995). We have shown above that local actin bundle loss preceded local lamellipodial retraction. The controlled application of collapsing factor and time-lapse imaging provided the opportunity to directly test how local actin bundle loss affected lamellipodial dynamics during ML-7–induced turning. We compared the lamellipodial area facing away from the ML-7 gradient with that facing the ML-7 during the turning process. This analysis was limited to conditioned medium growth cones that maintained well-extended lamellipodia during the turning process. Results showed that asymmetrical lamellipodial protrusion away from the ML-7 gradient always preceded bending of the neurite shaft (turning; Fig. 5, a and b). This indicates that actin filament reorganization in the lamellipodium occurs before microtubule changes that cause neurite bending.

To test whether actin bundle loss underlies this asymmetrical lamellipodial protrusion, we next examined the effect of ML-7 on polylysine-attached growth cone lamellipodial protrusion when bath applied. There is marked lamellipodial protrusion during polylysine-attached growth cone formation after axotomy (Welnhofer et al., 1997). In

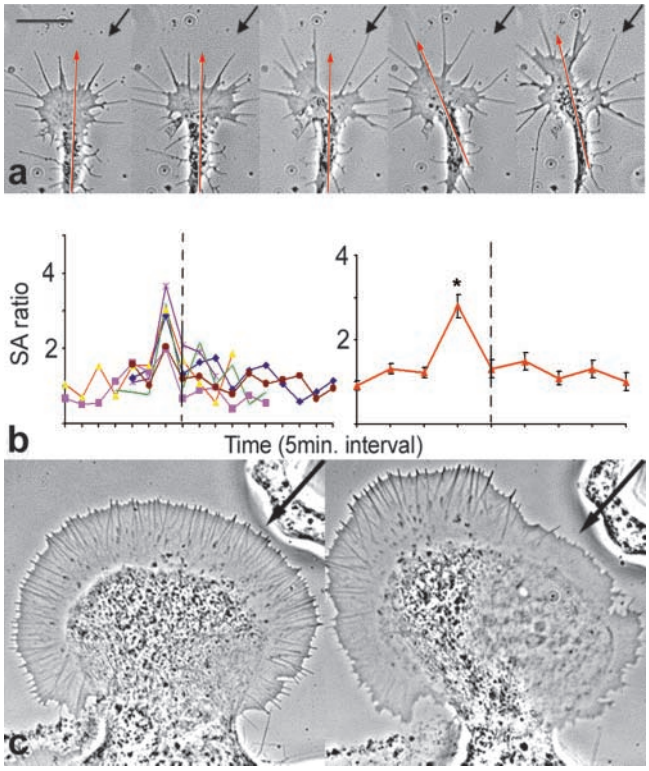

Figure 5. **Local actin bundle loss induces asymmetrical lamellipodial protrusion correlated with repulsive turning.** (a) Time-lapse movies of repulsive turning of extending conditioned medium growth cones in response to local application of ML-7 (arrow indicates the direction of ML-7-release). (b) The ratio of growth cone surface area (SA ratio, see Materials and methods) was plotted against time for individual growth cones (b, left graph; $n = 6$). Plots are lined up by the frame in which the neurite shaft started to turn (a, frame 4; b, dotted line). Note that changes of neurite shaft direction (turning) were always preceded by asymmetrical lamellipodial protrusion away from the ML-7 (higher SA ratio). Statistical analysis of pooled data (b, right graph) showed that this biased protrusion before neurite turning was significantly different from that at time points when there was no turning ($P < 0.0001$). (c) Locally applying ML-7 to polylysine-attached growth cones (arrow indicates the position of the pipette) induced local actin bundle loss, which led to lamellipodial protrusion only in areas where actin bundles still remained. Bar, 10 μm.

controls, the lamellipodial area increased over time (66 ± 9.44%, from 45 min after axotomy to 90 min; $n = 16$). However, lamellipodial expansion in the presence of ML-7 (50 μM) was significantly less than the control (19 ± 4.98%; $n = 15$; $P < 0.0005$). LPA pretreatment, which antagonized ML-7–induced actin bundle loss, significantly rescued lamellipodial expansion (38 ± 5.35%; $n = 19$; $P < 0.05$). Thus, loss of actin bundles after ML-7 bath treatment stopped lamellipodial expansion. Subsequently, when ML-7 was applied locally to induce local actin bundle loss in polylysine-attached growth cones (Fig. 5 c), we observed that lamellipodia on the side where actin bundles remained protruded significantly more (31 ± 9.15%) than those on the side where actin bundle loss occurred (9 ± 2.80%; $n = 8$; $P < 0.05$). This coincided with asymmetrical protrusion and shifting of the C-domain in the same direction as lamellipodial protrusion, which is a characteristic event during growth cone steering (Suter et al., 1998). Controls showed no significant preferential lamellipodial expansion (11 ± 3.62% vs. 20 ± 6.45%; $P = 0.27$; $n = 9$). Together, based on our previous results that ML-7 does not affect actin dynamics, including both polymerization and retrograde flow (Zhou and Cohan, 2001), these data suggest that spatial regulation of actin bundles plays an important role in regulating lamellipodial protrusion and subsequent growth cone turning. This provides direct evidence that actin bundle reorganization is an initial event that leads to asymmetric lamellipodial protrusion, which is followed later by microtubule redistribution and subsequent axon bending.

Coordinated rearrangement of microtubule structure and lamellipodial dynamics during growth cone splitting

In some experiments, when actin bundles were lost in the middle of polylysine-attached growth cones (Fig. 6, a–c), lamellipodia protruded on both margins where actin bundles still remained. This was followed by splitting of the growth cone C-domain (Fig. 6 c), suggesting that local actin bundle loss in the middle of the growth cone may underlie growth cone splitting. This was confirmed by similar observations in some turning experiments of conditioned medium growth cones (Fig. 6, d–g). In some cases, local ML-7 caused lamellipodial retraction in the middle of the growth cone (Fig. 6, d and e), followed by lamellipodial protrusion on both sides, subsequent dividing of lamellipodia (Fig. 6 f), and growth cone splitting (Fig. 6 g). This was presumably due to a pipette position that caused a local effect in the middle rather than on one side. Consistent with this, local application of ML-7 in our turning experiments resulted in more frequent growth cone splitting compared with the control (31%; $n = 39$; $P < 0.01$ vs. 6%; $n = 32$). LPA pretreatment that antagonized ML-7's effect also inhibited ML-7–induced growth cone splitting (4%; $n = 23$; $P < 0.05$ vs. ML-7 alone). When the microtubule structure of a splitting growth cone was examined (Fig. 6, h–j), it showed that free dynamic microtubule ends were only present in regions where actin bundles remained and lamellipodial protrusion occurred (Fig. 6, i and j). Moreover, most of these dynamic microtubule ends overlapped with actin bundles (Fig. 6 j). Together, these results further confirmed that spatial regulation of actin bundles is an underlying mechanism that controls microtubule structure and lamellipodial dynamics.

Discussion

The main goal of this study was to test whether specific and localized disruption of an important cytoskeletal structure of growth cones, actin bundles, could affect growth cone steering. We present evidence that local actin bundle loss is sufficient to induce repulsive growth cone turning. Most importantly, we found that microtubule distribution in the growth cone P-domain was closely regulated by both actin bundle reorganization and actin dynamics, providing a potential mechanism that couples leading edge actin with microtubules in the C-domain during growth cone turning.

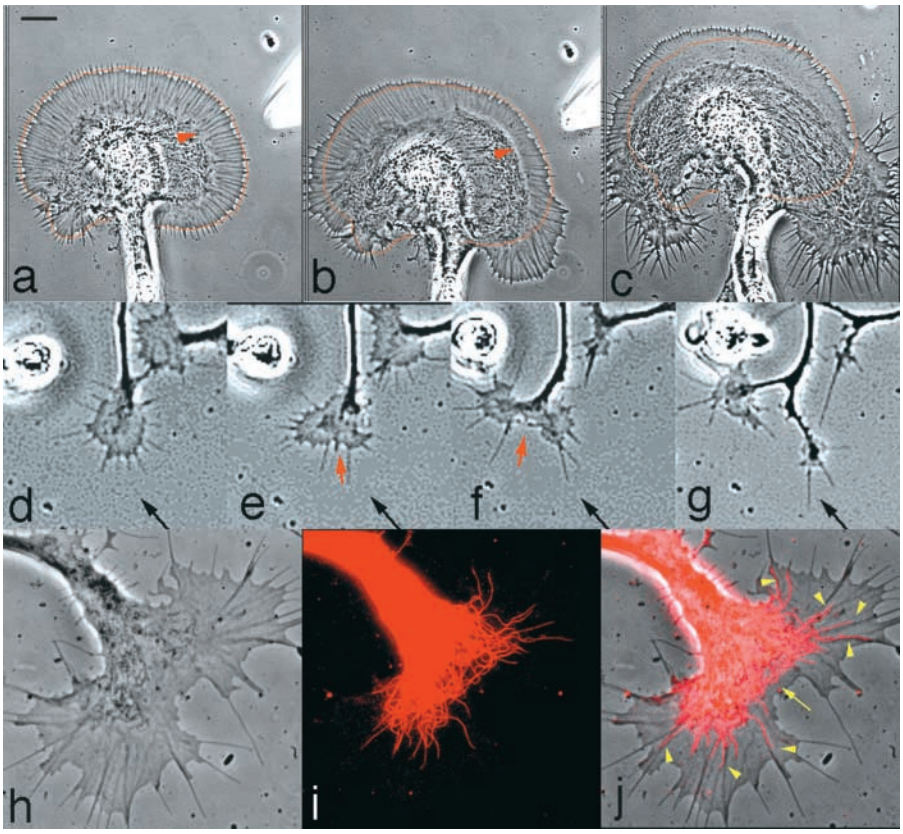

Figure 6. **Position of actin bundle loss determines lamellipodia dividing correlated with growth cone splitting.** Locally applying ML-7 to polylysine-attached growth cones caused actin bundle loss in the middle of the growth cone (a and b, red arrowhead). This led to lamellipodial protrusion on both margin areas where actin bundles still remained, as well as splitting of the growth cone C-domain (c). Local application of ML-7 (black arrows) to some conditioned medium growth cones (d) induced localized lamellipodial retraction and subsequent lamellipodia dividing (e and f, red arrows). This resulted in growth cone splitting (g). Examination of a splitting growth cone (h) showed that microtubule extension (i) was correlated with actin bundle changes and lamellipodial protrusion. Microtubules extended into areas where actin bundles remained (yellow arrowheads), but were absent in areas where actin bundles were lost (yellow arrow) in the middle of the lamellipodium (j). Note that the dynamic microtubule ends colocalized with actin bundles (j). Bar: (a–c) 5 μm; (d–g) 3.7 μm; (h–j) 10 μm.

ML-7 induces repulsive turning through local actin bundle loss

Filopodia and lamellipodia are two essential structures required for growth cone motility during axon guidance. Filopodia serve as sensory elements for guidance signals (Davenport et al., 1993). Actin bundles, the core elements of filopodia, span the whole lamellipodium to contact microtubules in the C-domain (Bridgman and Dailey, 1989). This unique feature of actin bundles fits very well with their potential role in mediating growth cone turning in response to guidance cues by coordinating actin filaments at the leading edge with microtubules in the C-domain.

To disrupt actin bundle structure, we used the MLCK inhibitor ML-7, which induced marked, repulsive growth cone turning when applied locally. Several lines of evidence have shown that specific disruption of actin bundle structure is the primary effect of ML-7. First, our previous study showed that ML-7 selectively induced actin bundle loss without affecting actin dynamics, including both actin polymerization and retrograde flow (Zhou and Cohan, 2001). Therefore, it is unlikely that a local change in actin dynamics (actin polymerization or retrograde flow) is the cause for ML-7–induced repulsive turning. The fact that LPA, which has been shown to antagonize ML-7–induced actin bundle loss, abolished turning further confirms the role of actin bundle loss in mediating repulsive growth cone turning. A possible mechanism of the LPA effect, as we discussed previously (Zhou and Cohan, 2001), is through activation of RhoA and subsequent Rho kinase, which then phosphorylates myosin light chain (Amano et al., 1996). Indeed, the involvement of myosin light chain phosphorylation has recently been shown to regulate axon stability in vivo (Billuart et al., 2001). Second, it is also unlikely that ML-7 directly affects microtubule structure and causes turning. This is supported by our result that loss of dynamic microtubules from the P-domain by vinblastin treatment had little impact on actin bundle structure, indicating that actin bundle loss by ML-7 treatment is not caused by microtubule loss. Moreover, we have never seen depletion of dynamic microtubules from the P-domain without actin bundle loss when treated with ML-7, suggesting that the loss of dynamic microtubules is a secondary effect of actin bundle loss (see below). Third, local actin bundle loss preceded the axon bending and growth cone turning shown in our conditioned medium cultures, further supporting its role as an initial event mediating turning. Fourth, based on our previous study, it is likely that ML-7 induces actin bundle loss by inactivating myosin II activity rather than by some other nonspecific effects. This is supported by a recent study of myosin IIB knockout mice, which resulted in the loss of actin bundles from growth cones (Bridgman et al., 2001). Last, similar changes in actin bundles and microtubules were also observed in response to a physiological guidance cue, serotonin, which suggests the generality of these cytoskeletal changes in turning. In summary, all evidence shown above supports actin bundle loss induced by ML-7 as a primary event that triggers repulsive turning.

Interestingly, ML-7 affected the proximal portion of actin bundles that traversed the lamellipodium more than the distal portion in filopodia. This may explain why some filopodia remained on the side of application. Similar effects were described previously in growth cones treated with TPA (Cohan et al., 2001), which increases phosphorylation of the ac-

tin bundling protein, fascin, and decreases its actin binding properties (Yamakita et al., 1996). Fascin localized to actin bundles in growth cones and showed a graded distribution, with antibody staining increasing distally along bundles. Similarly, the actin binding protein Mena is concentrated at the tip of the filopodia (Lanier et al., 1999). These findings suggest that actin binding proteins along filopodial actin bundles may be spatially regulated.

Spatial regulation of microtubules by the actin cytoskeleton

Coordinated changes in dynamic microtubules and actin filaments are crucial for growth cone steering during axon pathfinding (Bentley and O'Connor, 1994). Reduction of actin filaments from the growth cone in vivo abolishes its ability to turn (Chien et al., 1993). Similarly, growth cones without dynamic microtubules in the P-domain also lose their steering capacity (Challacombe et al., 1997). It is widely accepted that signals from guidance cues are first interpreted through actin reorganization, which then, in turn, induces directed microtubule protrusion to complete the turning process. However, the nature of the actin reorganization and how it regulates microtubules still remain elusive.

There are two potential hypotheses for the role of actin filaments in regulating microtubule distribution during growth cone turning. First, it has been suggested that F-actin has a negative role in regulating microtubule extension. For instance, depleting F-actin with cytochalasin B resulted in massive extension of microtubules into the growth cone P-domain, where microtubule density is usually low (Forscher and Smith, 1988; this paper), indicating actin filaments as physical barriers for microtubule extension. Our data indicate that the negative influence of the actin meshwork results from its retrograde flow rather than from the actin filaments themselves. Second, there is also evidence that actin bundles in the filopodia may capture, stabilize, and promote microtubule extension during the growth cone turning process (Gordon-Weeks, 1991). In support of this, growth cones treated with low concentrations of vinblastin or taxol, which prevent microtubule interaction with actin filaments without affecting its polymerization ability, are unable to turn to avoid inhibitory substrate (Williamson et al., 1996; Challacombe et al., 1997). Our results in this study show that F-actin can both prevent and promote microtubule extension depending on F-actin organization and dynamics in the P-domain. When actin filaments are organized into meshwork, F-actin powered by retrograde flow prevents extension of microtubules into the growth cone P-domain. A similar event has been shown in the leading edge of fibroblasts (Waterman-Storer and Salmon, 1997). In contrast, actin bundles selectively promote extension of some dynamic microtubules into the actin-rich domain. Reorganization of F-actin from bundles to meshwork by ML-7 without losing retrograde flow results in total depletion of microtubules, suggesting the essential role of actin bundles in promoting microtubule extension into the P-domain. Treating growth cones with BDM that inhibits actin retrograde flow allows microtubules to enter the P-domain in spite of the existence of a dense actin meshwork, suggesting that the physical existence of actin filaments alone cannot act as a barrier for microtubules. Thus, both actin filaments and retrograde flow are required to regulate microtubules in the P-domain.

Microtubule extension into the P-domain of growth cones is regulated by their plus end dynamics. Our results indicate that most microtubules are removed from the P-domain by microtubule transport via actin retrograde flow and microtubule depolymerization. Tracking of a subset of microtubules along actin bundles may promote the extension of these microtubules into the P-domain by directly affecting microtubule dynamics, such as by stabilizing microtubules and promoting their growth. This may occur through physical binding of actin bundles to microtubules through actin–microtubule cross-linking proteins. For instance, microtubule–actin cross-linking factor is located on microtubules in the actin-rich cortical region of epithelial cells (Fuchs and Karakesisoglou, 2001). Another microtubule plus end–binding protein, adenomatous polyposis coli , which can stabilize microtubules, indirectly binds actin filaments via β-catenin (Dikovskaya et al., 2001). In addition, several microtubule-associated proteins (MAPs) have both microtubule and actin binding activities (Seldon and Pollard, 1983; Togel et al., 1998; Ozer and Halpain, 2000). The localization of these proteins in growth cones will be of great interest for mechanistic insight into the regulation of microtubules by actin bundles.

Studies in fibroblasts have shown that microtubule dynamics also affect actin-based lamellipodial dynamics by regulating focal adhesions (Small et al., 1999). Targeting of microtubules to adhesion sites causes the dissociation of adhesion complexes and is associated with lamellipodial retraction (Kaverina et al., 1999). Lamellipodial collapse initiated by ML-7 is unlikely through microtubule-mediated relaxation of focal adhesions, because actin bundle loss induces retraction of microtubules away from the leading edge. However, microtubules that penetrate into the P-domain may regulate motility during protusion (Waterman-Storer et al., 1999).

Finally, repulsive turning may not require primary changes in retrograde flow that may result from altered interaction between growth cones and extracellular matrix proteins, which has been suggested as a potential mechanism of growth cone turning (Suter and Forscher, 1998). This is consistent with the fact that growth cones cultured on uncoated glass still turn in response to guidance cues (Ming et al., 1997), and growth cone turning can occur without asymmetrical growth cone–substrate adhesion (Isbister and O'Connor, 1999). Therefore, spatial regulation of microtubules by actin bundles provides an alternative mechanism for growth cone turning.

Proposed cytoskeletal model of repulsive growth cone turning

Our data provide direct evidence that local actin bundle loss on one side of the growth cone is sufficient to initiate repulsive turning. The ability of F-actin organization and dynamics to regulate the microtubule spatial distribution shown in this study provides a simple cytoskeletal mechanism that can be used to regulate growth cone turning. Localized guidance signals received by receptors on filopodia may influence actin bundles, either directly or though intermediate proteins, and

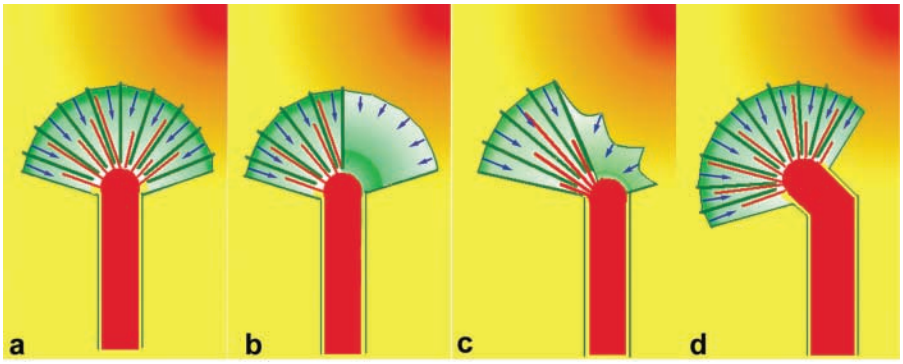

Figure 7. **Proposed cytoskeletal mechanism of repulsive growth cone turning.** (a) A typical growth cone has an actin-rich P-domain, which is organized into actin bundles (green lines) and actin meshwork that accumulates at the leading edge (green gradient), as well as a C-domain that contains microtubules (red). Under normal conditions, F-actin powered by retrograde flow (blue arrows) impedes microtubules from entering the growth cone P-domain. Meanwhile, actin bundles selectively promote the advancement of some microtubule ends (red lines) into the P-domain. (b) An extracellular gradient of repulsive cue (red–yellow gradient) induces a local actin bundle loss, which leads to the translocation of actin filaments from the leading edge to the center. (c) This results in asymmetrical lamellipodial protrusion and partial growth cone collapse. In the meantime, free microtubule ends are excluded from the area facing the repulsive cue due to actin bundle loss (b and c). (d) Lastly, lamellipodia protrude in the area where actin bundles remain, and microtubules overlapping with remaining actin bundles initiate directional extension and bundling, which causes the neurite to turn in the direction of lamellipodial protrusion.

cause asymmetrical actin bundle reorganization, which may subsequently orient microtubules. This will initiate asymmetrical extension of microtubules, followed by invasion of organelles along them, to complete the turning process. Our results support the following model for a cytoskeletal mechanism of repulsive growth cone turning. Under normal conditions, F-actin powered by retrograde flow impedes microtubules from entering the growth cone P-domain. Meanwhile, actin bundles selectively promote some microtubule ends advancing into the P-domain (Fig. 7 a). A signal from an extracellular gradient of repulsive cue induces a localized loss of actin bundles within growth cones (Fig. 7 b). Actin filaments from disassembled bundles contribute to the meshwork and trigger translocation of actin filaments away from the leading edge, which leads to partial growth cone collapse and asymmetrical lamellipodial protrusion (Fig. 7 c). In the meantime, microtubule ends in the P-domain are excluded from the area facing the repulsive cue due to actin bundle loss and subsequent collapsed meshwork around the C-domain. Lastly, microtubules overlapping with remaining actin bundles initiate directional extension and bundling, which causes the neurite to turn in the direction of lamellipodial protrusion (Fig. 7 d). This model is consistent with the findings that diminishing actin bundles with a low concentration of cytochalasin abolishes the turning ability of growth cones both in vitro (Challacombe et al., 1996) and in vivo (Chien et al., 1993). In addition, when actin bundle loss occurs in the middle of the growth cone, the growth cone bifurcates due to similar coordinated reorganization of F-actin and microtubules. Moreover, when growth cones advance linearly, actin bundle loss can be observed symmetrically on both sides at the lateral margins of the lamellipodium near the axon (unpublished data). Therefore, this provides a simple mechanism for the different behaviors of growth cones during their pathfinding, including regular advance, repulsive turning, and branching. This mainly involves spatial regulation of actin bundling and its subsequent effect on microtubule distribution and lamellipodial dynamics within growth cones.

Many of the physiological factors involved in axon guidance are able to affect actin bundling in growth cones. First, recent studies showed that growth cones from the snail *Lymnaea* could be guided by target-released dopamine and serotonin (Spencer et al., 2000; Koert et al., 2001), both of which cause similar collapse (McCobb et al., 1988) and actin bundle loss in *Helisoma* growth cones (Zhou and Cohan, 2001). This is supported by our result that serotonin induced the same microtubule reorganization as ML-7 upon actin bundle loss. Second, the neurite outgrowth inhibitor Nogo, which has been shown to induce growth cone collapse, also is associated with actin bundle loss (Bandtlow and Schwab, 2000). Third, a protein that binds Rho guanine exchange factor protein Trio, which plays an important role in axon guidance, colocalizes with myosin II and actin bundles (Seipel et al., 2001). Last, many common signal transduction molecules involved in axon guidance, such as calcium (Hong et al., 2000; Zheng, 2000), PKC (He et al., 1997), and tyrosine kinases (Wills et al., 1999), are all able to regulate actin bundling in growth cones (Goldberg and Wu, 1995; Zhou and Cohan, 2001). Taken together, this suggests that actin bundles are potential key factors that modulate growth cone motility in response to physiological guidance cues. Future work to identify molecules downstream of guidance cues that act on actin bundles, as well as molecules that regulate actin bundle–microtubule interaction, will be of great interest.

Materials and methods

ML-7 was purchased from Calbiochem-Novabiochem; BDM, serotonin, cytochalasin D, poly-L-lysine, and tubulin antibodies were from Sigma-Aldrich; Bodipy FL phallacidin was from Molecular Probes; LPA was from Cayman Chemical; salt-free Liebowitz L-15 medium was made by GIBCO BRL.

Cell culturing

For experiments conducted on polylysine-attached growth cones, neurons with attached axons were removed from the buccal ganglia of *Helisoma trivolvis* and cultured in defined medium L-15 on polylysine-coated coverslips. For growth cone turning experiments, neurons were cultured in the medium containing conditioning factors prepared from *Helisoma* brain (Zhou and Cohan, 2001). Cells were cultured for 8–12 h to allow for neurite outgrowth.

Video and fluorescent microscopy

Growth cones were viewed with an inverted light microscope (Nikon Diaphot) equipped with a dry condenser (0.52 NA) for phase contrast optics.

Images of growth cones were recorded with a cooled CCD camera (Photometrics Ltd.) controlled by IP Lab Spectrum software (Scanalytics) after 2.5× projection. A 40× oil immersion phase objective (1.30 NA) was used for polylysine-attached growth cones, and a 20× or 40× phase objective (0.75 NA) was used for conditioned medium growth cones. All image processing was done with IP Lab Spectrum and final images were prepared using Adobe Photoshop®. For fluorescent staining, cells were fixed and stained with Bodipy FL phalloidin for F-actin, and α-tubulin, acetylated tubulin, and tyrosine tubulin antibodies for microtubules (Sigma-Aldrich), as described previously (Welnhofer et al., 1997). After fluorescent labeling, growth cones were viewed with the fluorescent microscope system (NikonDiaphot 300), consisting of a 100×, 1.25 NA oil objective lens.

Microtubule dynamics

X-rhodamine–conjugated bovine brain tubulin was prepared as described by Waterman-Storer and Salmon, 1997. Neuronal cell bodies in cultures were injected with labeled tubulin (2–3 mg/ml) and coverslips were mounted in Rose chambers (Reider and Hard, 1990) using defined medium supplemented with 2 mg/ml glucose and 10 μl/ml oxyrase (Oxyrase, Inc.).

For visualization of microtubule dynamics, time-lapse FSM was performed on a spinning disk confocal microscope system. 568-nm light from a 2.5 W krypton–argon ion laser (Coherent) was selected with a four-channel acousto-optical tunable filter (AOTF; Neos Technologies) and was delivered by a single-mode fiberoptic (Oz Optics) to the UltraView spinning disk confocal scan head (PerkinElmer) containing a reverse dichromatic mirror and emission filter for x-rhodamine fluorescence. The scanning point sources from the UltraView unit entered the side camera port of an inverted microscope (TE300 Quantum; Nikon) and were focused on the specimen through a 100× 1.4 NA Plan-Apochromatic DIC objective lens. The emission light from the specimen was collected by an Orca 2 camera (Hamamatsu, Inc.) operated in the slow-scan (1.25 mHz), 14 bit-depth mode. Images were collected at 10-s intervals using acquisition times of 0.5–1 s. Microscope functions and image analysis were controlled by MetaMorph software (Universal Imaging Corp.).

For image analysis, the distance between a fluorescent speckle along the microtubule lattice and the terminal microtubule speckle was measured in each calibrated image of the time-lapse series. The differences in this distance between each image in the series (10-s interval) were used to calculate instantaneous growth velocities. Retrograde flow rates were calculated independently by tracking the movement of individual speckles in consecutive images.

Measurement and data analysis

For the growth cone turning assay, the turning angle was defined as the angle between the original growth cone advancing direction and a line that connects growth cones before and after a 1-h exposure to the gradient (Song et al., 1997). The growth cone advancing direction was represented by drawing a line that overlapped the trailing axon behind the growth cone. To determine growth cone advance, the neurite extension trajectory was traced and measured with IP Lab software. Only growth cones that did not split and advanced more than 6 μm during a 1-h period were included in this study.

To measure lamellipodial expansion during growth cone formation, lamellipodia surface areas were measured with IP Lab software. To analyze lamellipodial dynamics during growth cone turning, only growth cones with well-extended lamellipodia through the whole turning process that made clear repulsive turns were included in the final analysis. Growth cones were divided in half by a line in the direction of neurite outgrowth, which overlapped the neurite shaft right behind the growth cone (Fig. 2 a). The ratio of growth cone surface area (area facing away from ML-7/area facing the ML-7) was calculated in each frame. Because the growth cone was very dynamic, the dividing line was adjusted in each frame so that it always overlapped the direction of the neurite shaft. During repulsive growth cone turning, this line rotated gradually away from the ML-7 gradient. To measure asymmetrical lamellipodial protrusion of polylysine-attached growth cones, growth cone images first were divided into roughly equal halves and the surface area of each half was measured (Fig. 2 c). Subsequent expansion of lamellipodia was represented as a percentage change of lamellipodial area between 45 and 90 min after axon severing. In addition, retrograde flow was measured by dropping polystyrene beads onto the surface of polylysine-attached growth cones before and after application of BDM, as previously reported (Welnhofer et al., 1997).

To quantify microtubule distribution in the polylysine-attached growth cone P-domain, the average fluorescent intensity (AFI) of microtubule and background staining within the actin-rich P-domain were measured. The adjusted microtubule AFI ($AFI_{P\text{-}domain} - AFI_{background}$) was then normalized by the AFI of single microtubules identifiable in the P-domain. The obtained ratio $R = (AFI_{microtubules} - AFI_{background}) / AFI_{single\ microtubule}$ represents the percentage of fluorescence in each growth cone P-domain contributed by single microtubule staining. For microtubules in conditioned medium growth cones, the percentage of growth cones with at least two identifiable free microtubule ends was calculated because ML-7–collapsed growth cones often contained one single free microtubule end associated with remnant filopodia.

All data were reported as mean ± SEM, and we used an unpaired *t* test to determine the significance of the data between groups. For multiple group comparison, one-way ANOVA was used followed by least significant decision (LSD) as post-hoc analysis. For percentage data, the Chi square test was used.

Online supplemental material

An example of microtubule dynamics in a polylysine-attached growth cone is available as a Quicktime movie (Video 1). Speckled microtubules in the P-domain can be observed under the influence of retrograde flow. Online supplemental material is available at http://www.jcb.org/cgi/content/full/jcb.200112014/DC1.

We thank Dr. Paul Torreano (University at Buffalo) for help with microtubule staining.

This work was supported by grants from the National Institutes of Health and National Science Foundation to C.S. Cohan and the Mark Diamond Research Fund of the Graduate Student Association at the State University of New York to F.-Q. Zhou.

Submitted: 4 December 2001
Revised: 26 March 2002
Accepted: 23 April 2002

References

Amano, M., M. Ito, K. Kimura, Y. Fukata, K. Chihara, T. Nakano, Y. Matsumura, and K. Kaibuchi. 1996. Phosphorylation and activation of myosin by Rho-associated kinase (Rho-kinase). *J. Biol. Chem.* 271:20246–20249.

Bandtlow, C.E., and M.E. Schwab. 2000. NI-35/250/nogo-a: a neurite growth inhibitor restricting structural plasticity and regeneration of nerve fibers in the adult vertebrate CNS. *Glia.* 29:175–181.

Bentley, D., and T.P. O'Connor. 1994. Cytoskeletal events in growth cone steering. *Curr. Opin. Neurobiol.* 4:43–48.

Billuart, P., C.G. Winter, A. Maresh, X. Zhao, and L. Luo. 2001. Regulating axon branch stability: the role of p190 RhoGAP in repressing a retraction signaling pathway. *Cell.* 107:195–207.

Bridgman, P.C., and M.E. Dailey. 1989. The organization of myosin and actin in rapid frozen nerve growth cones. *J. Cell Biol.* 108:95–109.

Bridgman, P.C., S. Dave, C.F. Asnes, A.N. Tullio, and R.S. Adelstein. 2001. Myosin IIB is required for growth cone motility. *J. Neurosci.* 21:6159–6169.

Challacombe, J.F., D.M. Snow, and P.C. Letourneau. 1996. Actin filament bundles are required for microtubule reorientation during growth cone turning to avoid an inhibitory guidance cue. *J. Cell Sci.* 109:2031–2040.

Challacombe, J.F., D.M. Snow, and P.C. Letourneau. 1997. Dynamic microtubule ends are required for growth cone turning to avoid an inhibitory guidance cue. *J. Neurosci.* 17:3085–3095.

Chien, C.B., D.E. Rosenthal, W.A. Harris, and C.E. Holt. 1993. Navigational errors made by growth cones without filopodia in the embryonic *Xenopus* brain. *Neuron.* 11:237–251.

Cohan, C.S., J.A. Connor, and S.B. Kater. 1987. Electrically and chemically mediated increases in intracellular calcium in neuronal growth cones. *J. Neurosci.* 7:3588–3599.

Cohan, C.S., E.A. Welnhofer, L. Zhao, F. Matsumura, and S. Yamashiro. 2001. Role of actin bundling protein fascin in growth cone morphogenesis: localization in filapodia and lamellipodia. *Cell Motil. Cytoskeleton.* 48:109–120.

Davenport, R.W., P. Dou, V. Rehder, and S.B. Kater. 1993. A sensory role for neuronal growth cone filopodia. *Nature.* 361:721–724.

Dikovskaya, D., J. Zumbrunn, G.A. Penman, and I.S. Nathke. 2001. The adenomatous polyposis coli protein: in the limelight out at the edge. *Trends Cell Biol.* 11:378–384.

Fan, J., and J.A. Raper. 1995. Localized collapsing cues can steer growth cones without inducing their full collapse. *Neuron.* 14:263–274.

Fan, J., S.G. Mansfield, T. Redmond, P.R. Gordon-Weeks, and J.A. Raper. 1993. The organization of F-actin and microtubules in growth cones exposed to a

brain-derived collapsing factor. *J. Cell Biol.* 121:867–878.

Forscher, P., and S.J. Smith. 1988. Actions of cytochalasins on the organization of actin filaments and microtubules in a neuronal growth cone. *J. Cell Biol.* 107:1505–1516.

Fuchs, E., and I. Karakesisoglou. 2001. Bridging cytoskeletal intersections. *Genes Dev.* 15:1–14.

Gallo, G., and P.C. Letourneau. 2000. Neurotrophins and the dynamic regulation of the neuronal cytoskeleton. *J. Neurobiol.* 44:159–173.

Goldberg, D.J., and D.Y. Wu. 1995. Inhibition of formation of filopodia after axotomy by inhibitors of protein tyrosine kinases. *J. Neurobiol.* 27:553–560.

Gordon-Weeks, P.R. 1987. The cytoskeletons of isolated, neuronal growth cones. *Neuroscience.* 21:977–989.

Gordon-Weeks, P.R. 1991. Evidence for microtubule capture by filopodial actin filaments in growth cones. *Neuroreport.* 2:573–576.

He, Q., E.W. Dent, and K.F. Meiri. 1997. Modulation of actin filament behavior by GAP-43 (neuromodulin) is dependent on the phosphorylation status of serine 41, the protein kinase C site. *J. Neurosci.* 17:3515–3524.

Hong, K., M. Nishiyama, J. Henley, M. Tessier-Lavigne, and M. Poo. 2000. Calcium signalling in the guidance of nerve growth by netrin-1. *Nature.* 403:93–98.

Isbister, C.M., and T.P. O'Connor. 1999. Filopodial adhesion does not predict growth cone steering events in vivo. *J. Neurosci.* 19:2589–2600.

Kaverina, I., O. Krylyshkina, and J.V. Small. 1999. Microtubule targeting of substrate contacts promotes their relaxation and dissociation. *J. Cell Biol.* 146: 1033–1044.

Koert, C.E., G.E. Spencer, J. van Minnen, K.W. Li, W.P. Geraerts, N.I. Syed, A.B. Smit, and R.E. van Kesteren. 2001. Functional implications of neurotransmitter expression during axonal regeneration: serotonin, but not peptides, auto-regulate axon growth of an identified central neuron. *J. Neurosci.* 21: 5597–5606.

Lanier, L.M., M.A. Gates, W. Witke, A.S. Menzies, A.M. Wehman, J.D. Macklis, D. Kwiatkowski, P. Soriano, and F.B. Gertler. 1999. Mena is required for neurulation and commissure formation. *Neuron.* 22:313–325.

Letourneau, P.C. 1983. Differences in the organization of actin in the growth cones compared with the neurites of cultured neurons from chick embryos. *J. Cell Biol.* 97:963–973.

Lin, C.H., E.M. Espreafico, M.S. Mooseker, and P. Forscher. 1996. Myosin drives retrograde F-actin flow in neuronal growth cones. *Neuron.* 16:769–782.

Lin, C.H., and P. Forscher. 1993. Cytoskeletal remodeling during growth cone–target interactions. *J. Cell Biol.* 121:1369–1383.

McCobb, D.P., P.G. Haydon, and S.B. Kater. 1988. Dopamine and serotonin inhibition of neurite elongation of different identified neurons. *J. Neurosci. Res.* 19:19–26.

Ming, G.L., H.J. Song, B. Berninger, C.E. Holt, M. Tessier-Lavigne, and M.M. Poo. 1997. cAMP-dependent growth cone guidance by netrin-1. *Neuron.* 19:1225–1235.

Ozer, R.S., and S. Halpain. 2000. Phosphorylation-dependent localizable of microtubule-associated protein MAP2c to the actin cytoskeleton. *Mol. Biol. Cell.* 11: 3573–3587.

Reider, C.L., and R. Hard. 1990. Newt lung epithelial cells: cultivation, use, and advantages for biochemical research. *Intl. Rev. Cytol.* 122:153–220.

Seldon, S.C., and T.D. Pollard. 1983. Phosphorylation of microtubule-associated proteins regulates their interaction with actin filaments. *J. Biol. Chem.* 258:7064–7071.

Seipel, K., S.P. O'Brien, E. Iannotti, Q.G. Medley, and M. Streuli. 2001. Tara, a novel F-actin binding protein, associates with the Trio guanine nucleotide exchange factor and regulates actin cytoskeletal organization. *J. Cell Sci.* 114:389–399.

Small, J.V., I. Kaverina, O. Krylyshkina, and K. Rottner. 1999. Cytoskeleton cross-talk during cell motility. *FEBS Lett.* 452:96–99.

Song, H.J., and M.M. Poo. 1999. Signal transduction underlying growth cone guidance by diffusible factors. *Curr. Opin. Neurobiol.* 9:355–363.

Song, H.J., G.L. Ming, and M.M. Poo. 1997. cAMP-induced switching in turning direction of nerve growth cones. *Nature.* 388:275–279 (erratum published 389:412).

Spencer, G.E., K. Lukowiak, and N.I. Syed. 2000. Transmitter–receptor interactions between growth cones of identified lymnaea neurons determine target cell selection in vitro. *J. Neurosci.* 20:8077–8086.

Suter, D.M., and P. Forscher. 1998. An emerging link between cytoskeletal dynamics and cell adhesion molecules in growth cone guidance. *Curr. Opin. Neurobiol.* 8:106–116.

Suter, D.M., and P. Forscher. 2000. Substrate–cytoskeletal coupling as a mechanism for the regulation of growth cone motility and guidance. *J. Neurobiol.* 44:97–113.

Suter, D.M., L.D. Errante, V. Belotserkovsky, and P. Forscher. 1998. The Ig superfamily cell adhesion molecule, apCAM, mediates growth cone steering by substrate–cytoskeletal coupling. *J. Cell Biol.* 141:227–240.

Tanaka, E., and J. Sabry. 1995. Making the connection: cytoskeletal rearrangements during growth cone guidance. *Cell.* 83:171–176.

Tessier-Lavigne, M., and C.S. Goodman. 1996. The molecular biology of axon guidance. *Science.* 274:1123–1133.

Togel, M., G. Wiche, and F. Prospt. 1998. Novel features of the light chain of microtubule-associated protein MAP1B: microtubule stabilization, self interaction, actin filament binding, and regulation by the heavy chain. *J. Cell Biol.* 143:695–707.

Waterman-Storer, C.M., A. Desai, J.C. Bulinski, and E.D. Salmon. 1998. Fluorescent speckle microscopy, a method to visualize the dynamics of protein assemblies in living cells. *Curr. Biol.* 8:1227–1230.

Waterman-Storer, C.M., and E.D. Salmon. 1997. Actomyosin-based retrograde flow of microtubules in the lamella of migrating epithelial cells influences microtubule dynamic instability and turnover and is associated with microtubule breakage and treadmilling. *J. Cell Biol.* 139:417–434.

Waterman-Storer, C.M., R.A. Worthylake, B.P. Liu, K. Burridge, and E.D. Salmon. 1999. Microtubule growth activates Rac1 to promote lamellipodial protrusion in fibroblasts. *Nat. Cell Biol.* 1:45–50.

Welnhofer, E.A., L. Zhao, and C.S. Cohan. 1997. Actin dynamics and organization during growth cone morphogenesis in *Helisoma* neurons. *Cell Motil. Cytoskeleton.* 37:54–71.

Williamson, T., P.R. Gordon-Weeks, M. Schachner, and J. Taylor. 1996. Microtubule reorganization is obligatory for growth cone turning. *Proc. Natl. Acad. Sci. USA.* 93:15221–15226.

Wills, Z., J. Bateman, C.A. Korey, A. Comer, and D. Van Vactor. 1999. The tyrosine kinase Abl and its substrate enabled collaborate with the receptor phosphatase Dlar to control motor axon guidance. *Neuron.* 22:301–312.

Yamakita, Y., S. Ono, F. Matsumura, and S. Yamashiro. 1996. Phosphorylation of human fascin inhibits its actin binding and bundling activities. *J. Biol. Chem.* 271:12632–12638.

Zheng, J.Q. 2000. Turning of nerve growth cones induced by localized increases in intracellular calcium ions. *Nature.* 403:89–93.

Zhou, F.-Q., and C.S. Cohan. 2001. Growth cone collapse through coincident loss of actin bundles and leading edge actin without actin depolymerization. *J. Cell Biol.* 153:1071–1084.